СПИСАНИЕ НА БЪЛГАРСКОТО ГЕОЛОГИЧЕСКО ДРУЖЕСТВО,
год. 82, кн. 2, 2021, с. 91–104

REVIEW OF THE BULGARIAN GEOLOGICAL SOCIETY,
vol. 82, part 2, 2021, p. 91–104

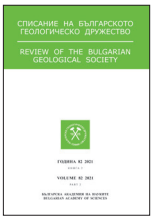

Българската геология и българските геолози в чужбина

Резюмета на статии в чуждестранни издания, излезли през 2019–2021

2019

Dekov, V. M., V. Y. Darakchieva, K. Billström, D. Garbe-Schönberg, G. D. Kamenov, M. Gallinari, L. Dimitrov, O. Ragueneau, E. Kooijman. 2019. Element enrichment and provenance of the detrital component in Holocene sediments from the western Black Sea. – *Oceanologia*, *62* (2); DOI: 10.1016/j.oceano.2019.10.001.

Concentrations of a large set of major and trace elements, and Sr, Nd and Pb isotope ratios were measured in Holocene sediments cored in the western deep Black Sea in order to unravel: (1) the controls of element enrichment, and (2) sources of the detrital component. The transition of the basin from oxic to euxinic resulted in enrichment or depletion in a number of elements in the deep-sea sediments. Authigenic Fe enrichment appears to depend on the amount of Fe mobilized from the sediment through the benthic redox shuttle mechanism and free H_2S in the water column (degree of "euxinization"). Manganese enrichment is controlled by diagenetic reactions within the sediment: the dissolution of Mn minerals, Mn^{2+} diffusion upward and reprecipitation. Barium enrichment is also controlled by diagenetic reactions, sulfate reduction and methanogenesis, that take place above and below the sulfate-methane transition, respectively. The major part of V, Co, Ni, Cu, Zn, Cr, Mo, Cd, and Sb is inferred to have co-precipitated with Fe in the euxinic deep waters and to have been incorporated into authigenic Fe-sulfides. Basin reservoir effect additionally influences the Mo enrichment. The U enrichment is interpreted to have a different origin in the two organic-rich stratigraphic units (II and I). It is inferred to be: (i) at the expense of the U inventory of the deepwater pool and a result of inorganic reduction of U at euxinic conditions in the lower Unit II; and (ii) at the expense of the U inventory of the surface water pool and a result of biogenic uptake and transfer to the sediment by the plankton in the upper Unit I. The high field strength elements are closely linked to the detrital component and their depletion in the organic-rich sediments reflects a dilution of the detrital component by the biogenic one. The enrichments of REE, Sn and Th are likely controlled by adsorption on clay minerals. Sr-Nd-Pb isotope compositions of the alumino-silicate component of the studied sediments are relatively uniform. They are most likely controlled by riverine suspended matter supplied mainly in the NW Black Sea (Danube Delta) and transported southward by marine currents, and to a lesser degree by suspended matter from the small rivers draining SE Bulgaria and NW Turkey. Wind-blown dust from the Sahara Desert appears to have a minor contribution to the alumino-silicate component of the sediments. The slight shift in the Pb isotopes in Unit I upper layers is possibly caused by the addition of anthropogenic Pb.

Kostov, R. I. 2019. Archaeological mineralogy and the dawn of gemmology: prehistoric (7th-5th millennium BC) gem minerals and gold from the Balkans (South-East Europe). – *J. Gems and Gemmology*, *21*, 4, 25–35; DOI: 10.15964/j.cnki.027jgg.2019.94.004.

The territory of the Balkan Peninsula in SE Europe is reviewed in European prehistory from the point of gemmology as the cradle of gem and decorative minerals and metals. During the local Neolithic period (end of 7th–6th millennium BC) as material for tools or for beads, pendants and idols are introduced nephrite (with the earliest known Balkan nephrite culture), jadeite-omphacite and quartz (different varieties). From the Chalcolithic period (5th millennium BC) are known large quantities of copper and gold artifacts (unique for the region; largest in number of gold artifacts is the Varna I Chalcolithic necropolis in Bulgaria). Among the gemmological materials on the Balkans are known malachite, antigorite serpentinite, turquoise, rock crystal, carnelian, jasper, jet and obsidian. In the Varna I necropolis (mid 5th millennium BC) are recorded the first known complex faceted carnelian beads with 32 facets, as well as some of the most important gemmological techniques and procedures as faceting, tumbling, annealing, miniaturization and standardization. As pigments for pottery in different pre-

historic sites are used cinnabar, graphite and gold. The earliest salt production on the Balkans is known form sites in Romania and Bulgaria, and because of its trade, salt is positively linked to a population rich with prestigious goods. The introduced possible Chalcolithic weight unit "van" (2 carats) is supposed to be the earliest known in prehistoric times.

Pavlishina, P., D. Dochev, V. Nikolov, M. Yaneva, R. Konyovska. 2019. Palynostratigraphy of dinosaur bone-bearing deposits from the Upper Cretaceous of Western Bulgaria. – *Acta Geologica Polonica*, *69* (4), 617–626; DOI: 10.24425/agp.2019.126443.

Palynological investigation of the Vrabchov Dol locality (Western Bulgaria) which recently yielded fragmentary dinosaur bones attributed to the clade Titanosauria, reveals well-preserved sporomorph assemblages dominated by angiosperm pollen from the Normapolles group, spores and rare gymnosperms. The age assessment of the studied sequence is based on the diagnostic Normapolles species, such as Oculopollis orbicularis Góczán, 1964, Oculopollis zaklinskaiae Góczán, 1964, Krutzschipollis spatiosus Góczán in Góczán et al., 1967 and Krutzschipollis crassus (Góczán, 1964) Góczán in Góczán et al., 1967. The concurrent presence of these pollen species suggests a late Santonian-early Campanian age for the succession. The sporomorph association is encountered in a palynofacies dominated by continental elements, including translucent phytoclasts (tissues, wood remains and plant cuticles). The sedimentary succession shows no evidence of marine elements and a very low proportion of AOM that attests to deposition within a lagoonal to foreshore marine environment, with high continental input and short transportation. The vegetation in the studied area was primarily composed of a range of Normapolles-producing angiosperms and secondarily of pteridophyte spore-producing plants. Gymnosperms were rare. Such a vegetation pattern reflects a warm, seasonally dry climate during the late Santonian-earliest Campanian in the studied area. The dinosaurs inhabited a wet lowland area, probably rich in herbaceous plants.

Sinnyovsky, D., N. Kalutskova, N. Dronin, D. Sinnyovska, A. Medvedev, N. Telnova. 2019. Concepts of geoparks establishment in Bulgaria and their geothermal resources. – In: *IOP Conference Series: Earth and Environmental Science*, *367*, 012006; DOI: 10.1088/1755-1315/367/1/012006.

Bulgaria is the third country in the world by number of mineral springs after Japan and Iceland. The Bulgarian-Russian collaboration in geological, environmental and landscape conservation provided a new development of the methodology for identification, evaluation and characterization of geodiversity including their geotermal resources. Individual approach to the concepts of the national geoparks stressed on their scientific and geodiversity features, environmental conditions and economic premises by defining one major geopark theme and many minor topics. Regardless of their radically different themes, the geothermal activity in geoparks is the common feature, which provides them with a great balneological potential. The concept of Geopark "Iskar Canyon" is based on the remarkable geodiversity of the Iskar River Canyon with a number of wonderful landscapes and scenic outcrops of various rock types ranging from Precambrian to Quaternary. The concept of Geopark "Belogradchik Rocks" lies on the famous Lower Triassic sandstone pinnacles. Geopark "Rila" is based on its remarkable glacial landscapes - glacier valleys, cirques, moraines, arêtes and horns. The major theme of Geopark "Burgas Lakes" is related with the ancient sea-level changes and balneo-healing properties of their humus mud. The unifying theme of these geoparks is the high spa potential of their thermal springs that have been used since the Roman Age.

2020

Ajdanlijsky, G., A. E. Götz. 2020. Palaeosols from the Lower Triassic continental red beds of NW Bulgaria: Stratigraphic tool for interpretation of fluvial depositional sequences. – *Zeitschrift der Deutschen Gesellschaft für Geowissenschaften*, *171* (4), 481–502; DOI: 10.1127/zdgg/2020/0241.

Ferric and calcic palaeosols are characteristic features of the fluvial red beds of the Lower Triassic Petrohan Terrigenous Group exposed in the Western Stara Planina Mountains of northwestern Bulgaria. The detailed documentation of 34 outcrop sections enables to distinguish different types of palaeosols, and to interpret their formation during lowstand, transgressive and highstand phases of two fluvial depositional sequences. Lowstand deposits, representing braided river stages of the fluvial system, are characterised by reworked palaeosol products recorded as channel-floor lags or in-channel bars. In-situ ferric palaeosol profiles featuring good drainage are also present. With increasing accommodation space, anastomosing fluvial accumulation became dominant and immature ferric and calcic profiles formed. The profiles in proximal position to the channels evidence good drainage, while those from the interchannel flood plain in more distal position feature poor drainage which led to the development of gleyed profiles. The palaeosol maturity increases towards the top of transgressive deposits, best documented by palaeosols that formed in the overbank fines. The low accommodation rate during the highstand phase led again to intense channel reworking of the palaeosol profiles, documented in different types of accumulation in channel, levee and overbank settings. During the highstand phase abundant and mature (cumulative and multistory) palaeosol profiles developed.

Ajdanlijsky, G., A. Strasser, A. E. Götz. 2020. Sequence analysis, cyclostratigraphy and palynofacies of early Anisian carbonate ramp deposits, NW Bulgaria. – *Annales Societatis Geologorum Poloniae*, *90* (4), 347–379; DOI: 10.14241/asgp.2020.27.

A sequence- and cyclostratigraphic interpretation of early Anisian (Aegean) shallow-marine carbonate ramp deposits, exposed in outcrop sections west of Tserovo village, NW Bulgaria, is presented. The hierarchical pattern identified can be interpreted in terms of Milankovitch cyclicity with elementary sequences representing the precession (20-kyr) cycle, small-scale sequences the short eccentricity (100-kyr), and medium-scale sequences the long eccentricity (400-kyr) cycle. Palynology provides a robust stratigraphic framework. The study of sedimentary organic matter, revealing variations of terrestrial input, sorting and fragmentation of phytoclasts, and prominent acritarch peaks, allows the interpretation of environmental changes and contributes to the cyclostratigraphic and sequence-stratigraphic framework. The detailed documentation of syndepositional soft-sediment deformation structures confirms their laterally traceable distribution within the depositional sequences and makes them good palaeoenvironmental indicators. Anisian ramp systems of the western Tethyan realm thus were subjected to highly dynamic regimes, recording the interplay between sea-level changes in tune with orbital cycles and ramp morphology.

Benderev, A., S. Shanov, K. Kostov, I. Ivanov. 2020. Hydraulic constructions and facilities on karst in Bulgaria: repercussions influence and problems. – *Carbonates and Evaporites*, *35*, 18; https://doi.org/10.1007/s13146-020-00554-z.

The safety and accident free exploitation of hydraulic facilities depends on geological and hydrogeological conditions of terrains where they are built. Such facilities have one of the most serious problems when they are located in a karst environment. In Bulgaria, there have been a number of cases of refusal to build dam walls at the preliminary exploration, as well as complication of the initial projects after clarification of the karst features in the affected areas. In many cases, after the construction of the facilities, changes are identified in the hydrogeological conditions which, besides the karst water regime, also affect the activity of the karst processes. Selected examples of hydraulic facilities on the territory of Bulgaria, the problems encountered, and the implemented engineering solutions are presented. The accomplished studies, construction and exploitation of hydraulic facilities in the karst terrains of Bulgaria are a serious experience that can be used in future similar activities.

Dekov, V. M., J. B. Maynard, G. D. Kamenov, O. Rouxel, S. Lalonde, S. Juranov. 2020. Origin of the Oligocene manganese deposit at Obrochishte (Bulgaria): Insights from C, O, Fe, Sr, Nd, and Pb isotopes. – *Ore Geology Reviews*, *122* (1), 103550; DOI: 10.1016/j.oregeorev.2020.103550.

The large manganese (Mn) deposit at Obrochishte (NE Bulgaria) is part of a cluster of similar Lower Oligocene deposits located around present-day Black Sea. They collectively constitute the Earth's second largest endowment of Mn, after the Kalahari Manganese Field in Africa. We have employed a battery of isotopic techniques (C, O, Fe, Sr, Nd, Pb) to help understand the genesis of this deposit. Carbon isotope data indicates that some sections of the Mn-ore layer have diagenetic $MnCO_3$ mineralization, formed by reaction of Mn oxides with organic carbon (Corg), whereas other sections have $MnCO_3$ precipitated directly from the seawater column. Oxygen isotopes show that the high-grade Mn mineralization had seawater as the fluid source, whereas some lower-grade sections had a mix of ground water and seawater as fluid sources. Sr and Nd isotope values of ore leachates also indicate that the Mn deposition occurred in normal lower Oligocene seawater. Nd and Pb isotope values suggest that the clastic host sediments were sourced from continental bedrock rather than younger arc volcanic rocks to the west. Iron isotope composition of the Mn ore implies deposition in a redox-stratified basin, similar to the modern Black Sea, with much of the Fe sequestered in deep, anoxic-euxinic water as sulfides. Similar to the modern Black Sea, most of the detrital Fe was transferred from shallow oxic sediments into deep, anoxic-euxinic water by an "iron shuttle" and remobilized Mn sequestered in the upper suboxic water layer. However, during the Oligocene, the "iron shuttle" operated intermittently due to the chemocline falling mostly below the shelf break, thereby limiting the efficiency of the shuttle mechanism. We propose a model for the lower Oligocene strata in which intense weathering during the Eocene weathering phase produced a thick lateritic crust on the southern European continent. The drastic sea-level drop at the end of the Eocene initiated downcutting of streams through this weathered material, transferring Fe- and Mn-oxides to the redox-stratified Western Black Sea. Here, these oxides were partly or entirely dissolved in the suboxic (Mn-oxides partly, Fe-oxyhydroxides entirely dissolved) and anoxic-euxinic (Mn-oxides entirely dissolved, dissolved Fe^{2+} re-precipitated) water layers. Eventually, Fe was re-precipitated as sulfide in the deep anoxic-euxinic water, while Mn accumulated in the suboxic water layer. Transgression in the early Oligocene brought this Mn-rich water onto the shallow shelf where it precipitated as Mn-oxide, then converted to Mn-carbonates during early diagenesis. Some Mn was also contributed by submarine groundwater discharge. Further transgression brought lower-oxygen water onto the shelf and Mn-carbonate precipitated directly from the water column. The findings from this work provide insights about the unique Oligocene geochemical event in the region that lead to the formation of the 2nd largest cluster of Mn deposits in the world.

Dimowa, L., Y. Tzvetanova, O. Petrov, I. Piroeva, F. Ublekov. 2020. Powder XRD structural study of Ba^{2+} modified clinoptilolite at different stages of the ion exchange process conducted at two temperature regimes – room temperature and 90 °C. – *Minerals*, *10* (11), 938; DOI: 10.3390/min10110938.

Partial and almost complete barium exchange on clinoptilolite is performed and structurally studied for different durations (2 h, 24 h, 72 h, 168 h, 12 d, 22 d) at room temperature and 90 °C of the ion exchange process. Continuing ion exchange up to the 22nd day is proved by EDS analyses data and powder XRD (intensity changes of 020 and 200 peaks). Rietveld structure refinement was first performed on the maximum Ba exchanged clinoptilolite at 90 °C for 22 days (3.04 atoms per unit cell). Four barium positions and 9 H2O sites were refined. The split positions Ba2 and BaK (around M3 site in channel C) were found mostly occupied by 2.23 atoms per unit cell. The rest of refined samples showed different occupations of the positions of incoming Ba^{2+} and outgoing cations (Na+, Ca^{2+}, K+, Mg^{2+}) during ion exchange, describing extra-framework cationic movements, which are released easily without preferable directions. The exchanges at 90 °C and room temperature were found proceeding similarly up to the 2nd hour, but then at room temperature the process is slowed and at 22nd day 1.64 barium atoms per unit cell are structurally refined.

Kirov, G., L. Dimova, Ts. Stanimirova. 2020. Gallery character of porous space and local extra-framework configuration in the HEU-type structures. – *Micropor. Mesopor. Mater.*, *293*, 109792; https://doi.org/10.1016/j.micromeso.2019.109792.

Published powder diffraction data are analyzed to find the particularities of the aluminosilicate framework and the possible local extra-framework cation-water and water assemblages and their interactions. Contrary to the popular channel model, the porous space in the aluminosilicate framework is examined as a unified, continuous gallery structure between two tetrahedral layers "leaning" on parallel rows of diortho-groups of T2 tetrahedra. The local distribution of Al^{3+} determines the distribution in the gallery space of the extra-framework cations in agreement with their specific properties. The local cation-water complexes around the positions of the extra-framework cations and possible local water complexes are proposed based on the inter-atomic distances, occupation and the opportunities to simultaneously occupation of adjacent positions determined by the structural refinement, as well as the properties of cations (a charge, dimensions, hydration characteristics) and other considerations. The division of the averaged structure refined by diffraction, into its constituent local complexes, is a prerequisite of understanding crystal-chemical relations in the zeolite structure and its behavior in different natural and technological processes.

Korzhenkov, A. M., A. N. Ovsyuchenko, O. V. Dimitrov, T. Dimov, A. S. Lar'kov, B. Ranguelov, E. A. Rogozhin, S. N. Rodina. 2020. Traces of strong eneolithic and medieval earthquakes hitting the Durankulak archaeological settlement in Northeastern Bulgaria. – *J. Volcanol. and Seismol.*, *14*, 262–282; DOI: 10.1134/S0742046320040028.

We have conducted paleo- and archaeoseismological surveys in the Durankulak Eneolithic archaeological settlement in Northeastern Bulgaria, identifying many earthquake-related deformations of different ages. The ubiquitous presence of counterfort walls added to damaged original (nearly north-south) walls on the eastern side provides evidence of the first significant earthquake in Durankulak that seems to have occurred during Middle to Late Eneolithic time (4650–4100 B.C.). This seismic event made the north-south walls tilt westward, so that the ancient residents had to build counterfort walls to prevent the original walls from collapsing. However, the upper excavations in the archaeological settlement show that the next, later, seismic deformation induced a tilting and collapse of remains of the original walls eastward, producing a gap of a few tens of centimeters between the original walls and the counterfort walls. Afterwards the settlement was abandoned. It may be surmised that the later earthquake was stronger than the earlier one, which left room for reconstruction work. The local seismic intensity of the earlier earthquake seems to have been at least $I_l \geq$VIII, while the later event had $I_l \geq$IX on the MSK-64 scale. Considering that the masonry of both walls, the original and the counterfort ones, is about the same age, the time interval between the two seismic events must have been short, one or two hundred years. Nevertheless, the epicenters of both of these earthquakes were to different directions from Durankulak. The seismic motion (compressive waves and shocks) went from the west during the first earthquake and from the east during the second. The rupture zone of the first seismic event was obviously related (1) to an earthquake-generating zone in continental Bulgaria situated west of the archaeological settlement in question, or (2) to the Intramoesian active fault that was responsible for the large earthquake of 1444. The rupture zone of the second seismic event was nearby, in the coastal part of the Black Sea; the responsible feature seems to have been the Shabla-Kaliakra seismogenic zone. Considerable seismic deformations were also identified in structures on the southern slope of the island in a dwelling dating back to the First Bulgarian Kingdom (the 9th century A.D.). This seismic event produced distortions in the walls (in map view), sigmoidal patterns, as well as fractures and rotations in the walls. The local seismic intensity due to this earthquake is supposed to be at least $I_l \geq$VIII. The rupture zone of a third seismic event was likely to be nearby, in the coastal part of the Black Sea, and the responsible feature must have been the Shabla-Kaliakra seismogenic zone.

Kostov, R. I. 2020. Archaeomineralogy of turquoise in Eurasia. – In: Querré, G., S. Cassen, E. Vigier (Eds). *La parure en callaïs du Néolithique européen*. Archaeopress, Oxford, 387–396.

A review is made on the deposits, distribution and finds of turquoise $CuAl_6(PO4)_4(OH)_8.4H_2O$ from prehistoric times to the early medieval period on the territory spanning from Southeast Europe (Bulgaria, Eastern Rhodopes, Late Neolithic to Chalcolithic period, end of 6th–5th mill. BC) to Central Asia (1 – Kyzyl Kum desert area, Neolithic period, 6th mill. BC; 2 – Iranian plateau area). A Turquoise Route (replacing the Lazurite Route) throughout the centuries (with the Kyzyl Kum area as an earlier source area) can be introduced in Central Asia, supplying raw material and turquoise artefacts to the West and to the South. The Western European, Anatolian and Caucasus Mountains, Levant, Sinai Peninsula and Chinese turquoise-bearing areas are also mentioned with examples of turquoise artefacts. Some earlier turquoise finds (8–7th mill. BC) must also be studied by mineralogical methods for determination of their probable source. In Europe and Asia turquoise deposits or occurrences are reported from 33 countries. Six main genetic types of turquoise deposits are distinguished (Kuraminsk, Kyzyl Kum, Taushan, Kalmakir, Kioster and Sinai type), which are a base for further on mineralogical, geochemical and archaeomineralogical studies in order to fingerprint the source areas of the turquoise artefacts.

Kostov, R. I. 2020. The enigma of the polyhedron and five-fold symmetry in Dürer's "Melencolia I". – *Symmetry: Culture and Science*, *31*, 4, 417–424.

The engraving "Melencolia I" (1514) by the German artist Albrecht Dürer (1471–1528) is studied from a symmetry point of view. A review is made on the interpretation of the enigmatic polyhedron or crystal, one of the key elements of the composition, in comparison with some of the artist's geometrical sketches and a preliminary mirror symmetry drawing. Five-fold symmetry is suggested both for the polyhedron and specific angles or proportions, linked to the correspondent golden section.

Kostova, I., J. C. Hower, D. Apostolova, Q. Wei. 2020. Concentration, distribution, and mode of occurrence of mercury in Bulgarian high-sulphur coals. – *IOP Conf. Series: Earth and Environmental Sci.*, 609, 012043; DOI: 10.1088/1755-1315/609/1/012043.

The goal of this study is to determine the mercury content, distribution, and modes of occurrence in high-sulphur coals from the Maritza-West, Maritza-East, and Stanyantsi basins in Bulgaria. The investigation is based on 51 samples representing the whole coal beds. The average concentration of Hg for all studied samples is 0.34 ppm and the values vary from 0.07 to 1.20 ppm; the average is 6.8-times higher than the Hg value in the upper continental crust and 3.4-times higher than the average values for world coals. The highest average Hg concentration (0.57 ppm) was found in the Maritza-West samples, followed by the Maritza-East (0.30 ppm), and the Stanyantsi (0.15 ppm) lignite. These data correspond with the sulphur content, i.e, the highest Hg lignite has the highest S content. A weak positive correlation between Hg and the total and sulphide S and a negative correlation between Hg and the organic S content for the Maritza-West lignite were observed. It is suggested that the Hg is predominantly incorporated in pyrite, which is present in high amount in these coals. The tendency in the distribution of Hg and S forms for the Maritza-East and Stanyantsi basins shows that Hg may be closely connected with S-bearing organic compounds, especially for the Maritza-East lignite. Consequently, the main part of Hg in the high-S coals from the Maritza-East and Stanyantsi basins is closely connected with organic sulphur complexes and may be with inorganic matter other than sulphide minerals. The data determined from this study partially confirms the results for other high-S world coals reported earlier. For the typical high-S Maritza-West lignite it may be suggested that there is a strong connection between Hg and pyrite and especially with epigenetic pyrite infilling the coal veins and cleats, while for high-S Maritza-East and Stanyantsi lignite the Hg is predominantly incorporated in organic matter and especially in sulphur-bearing organic compounds.

Lihareva, N., O. Petrov, L. Dimowa, Y. Tzvetanova, I. Piroeva, F. Ublekov, A. Nikolov. 2020. Ion exchange of Cs^+ and Sr^{2+} by natural clinoptilolite from bi-cationic solutions and XRD control of their structural positioning. – *J. Radioanalytical and Nuclear Chemistry*, *323*, 1093–1102; DOI: 10.1007/s10967-020-07018-7.

Clinoptilolite from Bulgaria was tested for uptake towards Cs^+ and Sr^{2+} from bi-cationic solutions using batch technique. Contact time and cation concentrations were investigated, revealing minor difference in Cs^+ sorption from single and mixed solutions but clear difference in Sr^{2+} uptake. Kinetic data were fit with pseudo-second-order kinetic model. The Langmuir isotherm model provided best description of equilibrium ion-exchange data [q_{max} (mg/g) is 122.7 for Cs^+ and 21.50 for Sr^{2+}]. Desorption experiments show that cesium and strontium ions are retained strongly by clinoptilolite. Rietveld structure refinement showed that approximately four Cs^+ ions were exchanged versus one Sr^{2+} ion in clinoptilolite.

Mafra, C., H. Bouzahzah, L. Stamenov, S. Gaydardzhiev. 2020. Insights on the effect of pyrite liberation degree upon the acid mine drainage potential of sulfide flotation tailings. – *Applied Geochem.*, *123*; DOI: 10.1016/j.apgeochem.2020.104774.

A new insight into the way in which the mineralogical composition and texture (liberation) of sulfides govern

the geochemical behavior of the tailings in terms of acid mine drainage (AMD) generation is presented. Two samples were taken from Dundee Precious Metals Chelopech (DPM-Ch) tailings management facility (TMF). They were likewise subjected to flotation to recover reactive (liberated and partially liberated) pyrite whilst the unreacted (locked) pyrite was kept in the tailings fraction. Geochemical (static and kinetic) tests were performed on the collected samples and tailings after flotation. A scanning electron microscope based automated mineralogy system was used to characterize them in terms of modal mineralogy, liberation degree and particle size. The absolute acid-generating potential (AP) defined by the Sobek method most likely overestimates the effective AP when pyrite is locked into non–reactive gangue minerals. Hence, the locked pyrite may unfavorably lead to increased tailings management costs. Therefore, the automated mineralogy data was used to calculate the effective AP of the tailings taking into account pyrite grade and its liberation degree. Based on these findings, it could be assumed that the amount of lime required to neutralize the acidity produced by pyrite oxidation would be considerably reduced (in the studied case nearly 4 times) if environmental desulfurization by flotation is practiced and the liberation degree of the acid-producing minerals is taken into account.

Milakovska, Z., M. Stefanova, G. Vladislavov, P. Nikolov, S. Marinov. 2020. Palaeoenvironmental evaluation by geochemical proxies of fluvio-lacustrine core log from the Late Miocene–Pliocene Maritsa Iztok Basin, Bulgaria. – *Geol. J.*, *56* (6); https://doi.org/10.1002/gj.3858.

A sequence of three lignite seams and interlayering carbonaceous mudstone is characterized by geochemical proxies. The study is extended by the palaeoenvironmental details given by the fossil fauna (gastropods, ostracods, and fishes). The predominant minerals (quartz and kaolinite) and main oxide relations of the carbonaceous mudstone point to sand and clay washed from weathered and/or altered felsic rocks from the catchment area. The mudstone features to deposition from suspension in standing or slow to persistently moving fresh waters at the bottom of the core log, and slightly aerated, warm, fresh to low saline, acidic to alkaline waters on the top. Three communities of organisms are depicted. The first is the pre-swamp environment characterized by standing or slow moving fresh waters and detrital organic matter deposition. The second is the environment of swamp of detrital forest trunks. Depending on the climate and water table, the main forest communities are of trees of families Cupressaceae, Taxodiaceae, and Podocarpaceae accompanied by trees of family Betulaceae, and herbaceous plants. Different Sphagnum species are also abundant. The dry/cold environment is reflected in the herbaceous organic matter deposition. Polar terpenoids ratio differentiates slight climatic oscillations for the samples with a strong Gymnospermae dominance. The second coal seam development reflects the optimum tectonic conditions for peat growth in a cold and dry climate leading up to 25 m lignite deposition. The third is the moss swamp environment with very fluctuating elements. At the top of the log, a Sphagnum-dominated peat has developed.

Minchev, A., A. M. Korzhenkov, A. N. Ovsyuchenko, O. V. Dimitrov, A. S. Lar'kov, B. K. Ranguelov, E. A. Rogozhin, N. V. Andreeva. 2020. Deformations in the Episcopal basilica in Varna: Evidences of strong historical earthquakes in Northwestern Bulgaria. – *Izvestiya, Atmospheric and Oceanic Physics*, *56*, 1202–1217; DOI: 10.1134/S0001433820100072.

Our archeoseismological investigations in the Episcopal basilica in Varna have revealed signs of seismic deformations in its walls: numerous shifts, tilts, and rotations of the wall parts around the vertical axis, as well as subvertical through-going joints cutting several stone blocks. A cluster of (at least) three seismic events occurred for a hundred years (from the early 5th to the early 6th centuries AD). Judging by kinematic indicators in the basilica structures built of high-quality stone blocks, the source of seismic motions was located north-northeast of the basilica. Strong seismic oscillations propagated apparently from the southwest. The seismic sources were along seismically active faults localized north and south of Varna. The local seismic intensity of seismic oscillations could reach $I_I \leq 9$ on MSK-64 scale. The intensity of the seismic oscillations increased due to unfavorable ground conditions at the location of the basilica. These data should be taken into account when assessing the seismic hazard assessment of Varna to build a new map of seismic zoning of northeastern Bulgaria.

Nikolov, H., M. Atanasova-Zlatareva, P. Ivanov, B. Berov. 2020. Studying the slope deformations in a Bulgarian mountain by multitemporal DInSAR data processing. – In: *Proceeding Vol. 11533 of Conference "Image and Signal Processing for Remote Sensing XXVI"*; DOI: 10.1117/12.2573945.

This research is focused on registering the movements along the slope of the several slopes located on southwest of the mountain Stara Planina and establishing their average annual values. Currently at national level there are a low number of studies targeted at operational monitoring of the investigated slopes. These objects are quite specific for research since those kind of natural phenomena are inaccessible by other means or are quite dangerous to be investigated. On the other hand, the moving slopes are causing damages to infrastructural objects such as roads, bridges or power lines. Their behavior is difficult to forecast and for this reason they can be considered as natural hazards. Obtaining precise data for the single slope movements is done by in-situ investigations

such as geodetic acquisitions, terrestrial laser scanning, and geological observations, which all require financial resources and human effort. For this reason, we used remotely sensed data from satellite based SAR instruments processed using the DInSAR method in order to analyze the motions of single slope and to establish a technique for the investigation of mountain slopes. An advantage of the selected method is the possibility to register the vertical movements of the whole slope with centimeter accuracy. This approach is based on the free access to the SAR data and tools for their thematic processing provided by ESA. In this study an emphasis is put on the manner how the obstacles encountered during the interferometric processing (e.g. presence of vegetation or topography) have been overcome. From the downloaded set of SAR images covering the region created were two multitemporal InSAR data series from ascending and descending orbits of the satellite. The results from the autumn-winter pairs exhibited good correlation with the expected displacements along the studied slope having a magnitude of 0.8 m.

Stanciu, I., D. Ioane. 2019–2020. Active fault systems in the Shabla region (Bulgaria) as interpreted on geophysical and seismicity data. – *Rev. Roum. Géophys.*, *63–64*, 3–21.

Shabla region is located in NE Bulgaria and belongs from the tectonic point of view to the southeastern part of the Moesian Platform. The study area covers parts of the eastern slope of the North Bulgarian arch, having the Bulgarian-Romanian border to the north, Cape Kaliakra to the south, Dobrich city to the west, and the Black Sea shelf to the east. Block faulting, horsts and grabens of different rank are the typical structural features. The crustal-scale Intramoesian fault, considered to separate the Moesian Platform in two main compartments, reaches the Black Sea continental shelf in Shabla region, its path being ambiguously located on maps, as it does not outcrop. Analysis of regional seismicity data available from ROMPLUS Earthquake Catalogue and EMSC Earthquake Catalogue, integrated with available tectonic and geophysical data, as well as with geological, geomorphological and neotectonic field observations, offered the possibility to interpret W-E, NE-SW and NW-SE active fault systems within the study area and build the grounds for a much more comprehensive understanding of this region's tectonic.

Tzvetanova, Y., O. Petrov, Th. Kerestedjian, M. Tarassov. 2020. Quantitative phase analysis of skarn rocks by the Rietveld method using X-ray powder diffraction data. – *Minerals*, *10* (10), 894; DOI: 10.3390/min10100894.

The Rietveld method using X-ray powder diffraction data was applied to selected skarn samples for quantitative determination of the present minerals. The specimens include garnet, clinopyroxene-garnet, plagioclase-clinopyroxene-wollastonite-garnet, plagioclase-clinopyroxene-wollastonite, plagioclase-clinopyroxene-wollastonite-epidote, and plagioclase-clinopyroxene skarns. The rocks are coarse- to fine-grained and characterized by an uneven distribution of the constituent minerals. The traditional methods for quantitative analysis (point-counting and norm calculations) are not applicable for such inhomogeneous samples containing minerals with highly variable chemical compositions. Up to eight individual mineral phases have been measured in each sample. To obtain the mineral quantities in the skarn rocks preliminary optical microscopy and chemical investigation by electron probe microanalysis (EPMA) were performed for the identification of some starting components for the Rietveld analysis and to make comparison with the Rietveld X-ray powder diffraction results. All of the refinements are acceptable, as can be judged by the standard indices of agreement and by the visual fits of the observed and calculated diffraction profiles. A good correlation between the refined mineral compositions and the data of the EPMA measurements was achieved.

Zagorchev, I., D. K. Ivanova, K. Stoykova, D. Bassi. 2020. Priabonian–Rupelian olistostromal events in the Northeastern Aegean islands: correlation with the Thrace basin and the Rhodopes. – In: Ersoy, E. Y., C. Akal, Y. Y. Öztürk (Eds). *IESCA 2019, 7 International Earth Science Colloquium on the Aegean Region. Proceedings.* Izmir, Dokuz Eylül Univ., 5–10.

We report a major olistostromal event situated around the Priabonian/Rupelian boundary. It is manifested in the island of Samothraki simultaneously with the development of a carbonate reef, preceded and followed by flyschoid sedimentation. Olistostrome formation of approximately the same age is observed also in the SE part of the island of Lemnos. Comparisons with the Thracian basin and the Rhodopes hint at the links of olistostrome and mélange formation with an episode of carbonatic sedimentation brusquely disturbed by increased tectonic activity of regional importance.

2021

Apostolova, D., I. Kostova, A. Bechtel, M. Stefanova. 2021. PAHs in feed coals and fly ashes from coal-fired thermal power plants in Bulgaria. – *Intern. J. Coal Geol.*, *243* (012092), 103782; DOI: 10.1016/j.coal.2021.103782.

The first thorough study of PAHs in feed coals and FAs from combustion in six Bulgarian TPPs was done. Since coal-derived FAs are applied to many targets, it is imperative to enhance the knowledge for their geochemical composition and environmental impact. The gap of information on PAHs in feed coals and coal-derived FAs

has outlined the aim of the study: (i) to compare by geochemical proxy PAHs in feed coals and FAs generated in six Bulgarian TPPs; (ii) to track the changes in PAHs compositions with feed coal ranks and in different ESP rows; and (iii) to estimate the potential toxicity of FAs (if any). Extractable organic matter (EOM) was prepared. PAHs were isolated in aromatic fractions and quantified in μg/kg. The total PAHs for lignite feed coal are in the range 400–530 μg/kg and for FAs 0.30–12.60 μg/kg: for subbituminous feed coal, they are 4000 μg/kg, and for FAs, 1.10–32.50 μg/kg. For bituminous feed coals, they are – 860 μg/kg and 9305 μg/kg, and for FAs from both TPPs, they are several times lower, from 69.4 μg/kg to 103.3 μg/kg, for the five ESP rows of Varna TPP and from 100.4 to 182.20 μg/kg, for the three rows of ESPs of Russe TPP. The EOM for low rank feed coals is strongly dominated by coal biomarkers, i.e., perylene and phenyl substituted PAHs. Therefore, calculations and ratios based on PAHs compositions are done only for bituminous feed coals and their FAs. Combustion has resulted in a regular shift to lighter PAHs compared to the signature PAHs of feed coals. PAHs distributions in FAs are dominated by phenanthrene. Distribution profiles according to the number of aromatic cycles (R) in PAHs are dominated by three-ring (3R) PAHs > four-ring (4R) PAHs. Only in the last row of ESP from the Varna TPP is there evidence for the presence of heavier PAH, five-ring (5R) benzo[g,h,i]fluoranthene, trapped by the finest particulate matter. Relatively low PAHs concentrations determined for FAs are compared with the values for PAHs in soils according to the Bulgarian regulation.

Balkanska, E., I. Gerdjikov, S. Georgiev, A. Lazarova, W. Dörr, A. Kounov. 2021. Structural and geochronological constraints on the magmatic and tectonic events in the pre-Alpine basement of the central parts of the Balkan fold-thrust belt (Central Stara Planina Mountains, Bulgaria). – *Intern. J. Earth Sci.*; DOI: 10.1007/s00531-021-02011-1.

The north-vergent Balkan fold-thrust belt of the Balkanide orogen, extending from northeast Serbia to the Black Sea region, was formed during at least two Alpine compressional events. However, remnants of the Variscan orogen are still preserved in its western and central parts. In the central part (Central Stara Planina Mountains), two pre-Permian metamorphic complexes of contrasting metamorphic degrees, the low-grade Stara Planina and high-grade Sredna Gora complexes, are juxtaposed along a major Variscan tectonic zone and intruded by voluminous granitoids of previously unknown age. Here, we present an extensive structural and U-Pb (TIMS and LA-ICP-MS) geochronological analysis, constraining several magmatic and tectonic events in the pre-Alpine evolution of the area. For the first time, early Cambrian magmatism (531.7±1.5 Ma/519.4±2 Ma) is reported from a granite intruding the low-grade Stara Planina complex. The juxtaposition of the metamorphic complexes before 314 Ma was followed by a transpressional stage between 313 and 306 Ma. The last Variscan penetrative ductile deformation was associated with the final emplacement stages of the Ambaritsa sheet-like pluton at about 306 Ma under still ongoing compression. In addition, at least two post-Variscan magmatic pulses of granitoid magmatism (at ca. 306–304 Ma and 250 Ma) have been distinguished in the studied area. Later, Alpine ductile to brittle deformational events led to an additional reworking of the Variscan edifice.

Bonev, N., P. Filipov, R. Raicheva, R. Moritz. 2021. Evidence of late Palaeozoic and Middle Triassic magmatism in the Sakar-Strandzha Zone, SE Bulgaria: Regional geodynamic implications. – *Intern. Geol. Review*; DOI: 10.1080/00206814.2021.1917008.

Upper Palaeozoic granitoids, meta-granitoids and meta-volcanic rocks predominate in the metamorphic basement of the northern and western parts of the Sakar-Strandzha Zone (SASTZ) in Southeast Bulgaria, together with the subsidiary Triassic meta-granitoids and meta-volcanic rocks. Generally, igneous minerals and textures are preserved, except in the meta-granitoids and meta-volcanic rocks that experienced a low- to high-grade metamorphic overprint. The volcanic rocks have a peraluminous and high-K calc-alkaline composition, and the granitoids range between I- to S-type compositions, typical of volcanic arcs and syn-collisional settings. LILE and LREE-enrichment and Nb-Ta anomalies characterize the intrusive and extrusive rock suites. U-Pb zircon geochronology has yielded crystallization ages between 245 and 237 Ma for the majority of the studied igneous rocks, and between 297 and 295 Ma for a small group of igneous rocks. Lower Permian and Middle Triassic igneous suites of the northern and western SASTZ have similar compositions and a similar tectonic setting when compared to upper Carboniferous–lower Permian intrusive and extrusive suites of the adjacent Sakar unit of the SASTZ, confirming a common regional late Palaeozoic–early Mesozoic tectono-magmatic event. As the late Carboniferous–Permian to Middle Triassic magmatic arc components extend across the SASTZ, they trace the time-correspondent active continental margin along the Eurasian plate during subduction of the Paleotethys oceanic lithosphere. The late Palaeozoic Eurasian active continental margin magmatic arc evolution of the SASTZ can be linked with the Serbo-Macedonian-Rhodope zones to the southwest, where coeval meta-granitoids document the same geodynamic context. By contrast, the Triassic igneous suite of the SASTZ is unrelated to the Serbo-Macedonian-Rhodope zones, where Triassic meta-ophiolite and meta-granitoids record Neotethys rifting.

Dimitrov, L., N. Lihareva, Y. Tzvetanova, O. Petrov. 2021. Synthesis of phillipsite from perlite utilizing mother waters from wet gel EMT preparation and study of the

obtained zeolitic material as ion exchanger. – *Environ. Earth Sci.*, *80*, 86; https://doi.org/10.1007/s12665-021-09378-z.

In the present paper, a supplementary method was elaborated for synthesis of phillipsite from perlite utilizing mother waters from wet gel EMT preparation. The method is reproducible and cheap – synthesis was performed at mild conditions at 90 °C. One of the obtained phillipsite samples was tested as ion exchanger with solutions containing K^+, Cs^+ and Sr^{2+} for simulated radioactive fixation of these ions. The kinetics of ion exchange was adequately described by pseudo-second-order kinetic model equations. The obtained parameters for the ion exchange properties of the synthesized phillipsite show that this material could be used in the Cs^+ and Sr^{2+} removal in decontamination processes. Cation-exchange effectiveness was also tested for Cs^+ and Sr^{2+} solutions, contaminated with model nonionic surfactant Pluronic 123, which may appear as a municiple pollutant.

Dimowa, L., Y. Tzvetanova. 2021. Powder XRD study of changes of Cd^{2+} modified clinoptilolite at different stages of the ion exchange process. – *Minerals*, *11* (10):1130; DOI: 10.3390/min11101130.

Cadmium exchange on clinoptilolite is performed and structurally studied for different durations of the ion exchange process (2 h, 24 h, 72 h, 168 h, 12 days, 22 days) at room temperature and 90 °C. The distribution of Cd^{2+} ions in all samples is elucidated after exchange on clinoptilolite using powder XRD data processed by Rietveld structural software. Clinoptilolite is not selective for Cd cations, but at 90 °C the exchange is ~2.5 cations per unit cell. At RT it reaches ~1.25 cations per unit cell being twice as low. The obtained maximum exchanged sample for 22 days 90 °C was structurally refined in order to find the cadmium positions in the clinoptilolite voids. The structural refinements of the occupations of the incoming and outgoing cations give an idea of how the intracrystalline diffusion is processed. A good correlation between results obtained by structural refinement of the Cd-exchanged samples and the data of the EDS measurements was achieved.

Georgiev, S., P. Marchev, B. Jicha, B. Banushev, R. Raicheva, I. Peytcheva, A. von Quadt. 2021. $^{40}Ar/^{39}Ar$ age and petrology of magmatic rocks from East Balkan (Bulgaria) constrain the initiation of regional subduction in SE Europe. – *Lithos*, *398–399*, 106302; https://doi.org/10.1016/j.lithos.2021.106302.

A prominent subduction-related magmatic arc hosting significant mineralization formed in SE Europe during the Late Cretaceous. Previous studies on major magmatic centers and ore deposits suggested that this belt formed through southwards retreat of a subducting Neotethys oceanic slab. However, the timing and the petrologic characteristics of magmatic products from the less mineralized eastern portions of this belt remain largely unknown. The complete lack of radiometric ages and limited geochemical characterization of this magmatism adds considerable uncertainty on existing large-scale geodynamic reconstructions focused on the Late Cretaceous magmatism in SE Europe. Here, we address this question by studying little known Cretaceous lavas and sub-volcanic bodies from the Eastern Balkan, Bulgaria. Major and trace element contents of these volumetrically limited rocks show a clear subduction signature. The most primitive rocks are high-Al basalts, which further differentiated into andesites and dacites via fractional crystallization in relatively small magma chambers. The mineral chemistry and assemblages constrain magmatic conditions prior to crystallization to pressures of 3–7 kb, temperatures of 900–1020 °C, water contents of ~4–7 wt% and high oxygen fugacities. Phenocryst features like reverse zonation of clinopyroxene and amphibole and sieve and patchy textures of plagioclase suggest magma mixing processes. Initial εHf values of Cretaceous zircons (+2 to −2) and inherited, mainly Variscan and older zircons (+3 to −11) provide clear evidence for assimilation of crustal lithologies by mantle-derived Upper Cretaceous magmas. Amphibole phenocrysts from an andesite and a dacite give $^{40}Ar/^{39}Ar$ plateau ages of 94.67±0.40 Ma and 94.56±0.40 Ma, respectively. These dates are the oldest recorded in the entire Late Cretaceous magmatic belt and constrain the onset of the subduction magmatism to the later parts of the Cenomanian stage. Regional correlations based on these results reveal that processes of slab retreat were active also in the eastern part of the magmatic arc. Further, these results outline a clear temporal along-arc trend of progressively younger initiation of the arc magmatism from east to west.

González-Jiménez, J.-M., R. Piña, Th. N. Kerestedjian, F. Gervilla, I. Borrajo, J. Farré-de Pablo, J. A. Proenza, F. Tornos, J. Roqué, F. Nieto. 2021. Mechanisms for Pd-Au enrichment in porphyry-epithermal ores of the Elatsite deposit, Bulgaria. – *J. Geochem. Exploration*, *220*; https://doi.org/10.1016/j.gexplo.2020.106664.

Porphyry Cu can contain significant concentrations of platinum-group elements (PGE: Os, Ir, Ru, Rh, Pt, Pd). Inthis study, we provide a comprehensive in situ analysis of noble metals (PGE, Au, Ag) for (Cu-Fe)-rich sulfides from the Elatsite, one of the world's PGE-richest porphyry Cu deposits. These data, acquired using laser ablation inductively coupled plasma-mass spectrometry (LA-ICP-MS), indicate that Pd was concentrated in all the (Cu-Fe)-rich sulfides at ppm-levels, with higher values in pyrite (~6 ppm) formed at the latest epithermal stage (i.e., quartz-galena-sphalerite assemblage) than in bornite and chalcopyrite (<5 ppm) from the hypogene quartz-magnetite-bornite-chalcopyrite ores. Likewise,

Au is significantly more concentrated in pyrite (~5 ppm) than in the (Cu-Fe)-rich sulfides (≤0.08 ppm). In contrast, Ag reaches hundreds of ppm in pyrite and bornite (~240 ppm) but is in much lesser amounts in chalcopyrite (<25 ppm). The inspection of the time-resolved spectra collected during LA-IPC-MS analyses indicates that noble metals are present in the sulfides in two forms: (1) structurally bound (i.e., solid solution) in the lattice of sulfides and, (2) as nano- to micron-sized inclusions (Pd-Te and Au). These observations are further confirmed by careful investigations of the PGE-rich (Cu-Fe)- rich sulfides by combining high-spatial resolution of field emission scanning electron microscope (FESEM) and focused ion beam and high-resolution transmission electron microscopy (FIB/HRTEM). A typical Pd-bearing mineral includes the composition $PdTe_2$ close to the ideal merenskyite but with a distinct crystallographic structure, whereas Au is mainly found as native element. Our detailed mineralogical study coupled with previous knowledge on noble-metal inclusions in the studied ores reveals that noble metal enrichment in the Elatsite porphyry ores was mainly precipitated from droplets of Au-Pd-Ag telluride melt (s) entrained in the high-temperature hydrothermal fluid. These telluride melts could separate at the time of fluid unmixing from the silicate magma or already be present in the latter either derived from deep-seated crustal or mantle sources. Significant enrichment in Pd and Au (the latter correlated with As) in low-temperature pyrite is interpreted as remobilization of these noble metals from pre-existing hypogene ores during the epithermal overprinting.

Grabowski, J., K. Stoykova, H. Wierzbowski, P. Wójcik-Tabol. 2021. Upper Berriasian chemostratigraphy, clay minerals and calcareous nannofossils of the Barlya section (Western Balkan, Bulgaria): Implications for palaeoclimate and productivity changes, and stratigraphic correlations across the Alpine Tethys. – *Palaeogeography, Palaeoclimatology, Palaeoecology*, *567* (1), 110252; DOI: 10.1016/j.palaeo.2021.110252.

Upper Berriasian chemostratigraphic, clay mineral and calcareous nanofossil data are presented from a precisely dated hemipelagic section of Barlya (Western Balkan, Bulgaria). The section covers an interval from the upper part of the lower Berriasian (Calpionella elliptica Subzone, magnetozone M17r) to the lowermost Valanginian (Calpionellites darderi Subzone, magnetozone M14r). The study aims to reconstruct the major palaeoenvironmental changes (variations in lithogenic input, palaeoredox and palaeoproductivity) and their relation to palaeoclimate and regional tectonic regime, as well as their application to stratigraphic correlations with the Vocontian Basin and Jura Mts. A long-term increase in terrigenous input during the late Berriasian was controlled mostly by the orogenic activity in the NeoTethyan Collision Zone and to a lesser degree by climate humidification, as revealed by variations in kaolinite content and in lithogenic proxies (Ti/K, Th/K, Ti/Al and Zr/Rb ratios). A good correlation is observed between geochemical palaeoproductivity proxies (sedimentation rates of non-detrital (excess or authigenic) portions of P, Zn and Cd) and nannofossil fluxes, determined as the total abundance and species richness. Major calcareous nannofossil peaks, represented by high-diversity and high-abundance nannofossil assemblages, fall within the low-productivity intervals. A smaller peak formed by a low-diversity and high-abundance assemblage, dominated by *Watznaueria barnesiae/fossacincta*, coincides with the variable, but mostly high-productivity interval, which indicates high plasticity of *Watznaueria* concerning to environmental conditions. Additionally, trophic changes seem to correspond to bulk rock carbon-isotopic composition, with rising δ^{13}Ccarb values in more oligotrophic intervals. This offers perspectives for long-distance chemostratigraphic correlations between pelagic and platform sections, supplementing traditional schemes based on bio- and sequence stratigraphy. A holostratigraphic correlation is proposed between the Western Balkan (Barlya section), Vocontian Basin (Berrias and Monclus sections) and Jura Mts (La Chambotte section) based on bio-, magnetic and carbon-isotope stratigraphy, as well as climatic and palaeoproductivity proxies.

Gurova, M., P. Andreeva, E. Stefanova, A. Aladzhov, C. Bonsall. 2021. Petrographic and geochemical analyses of flint raw materials from Bulgaria: A reliable combination for provenance studies of archaeological flint. – *Quaternary International*; DOI: 10.1016/j.quaint.2021.03.023 (in press).

The Bulgarian prehistoric sequence is characterized by the use of particular raw materials in distinct 'cultural' contexts. The Karanovo I and II stages of the Early Neolithic (part of a supra-regional technocomplex in the Balkans) are recognisable by formal toolkits made of Balkan flint. The Chalcolithic period is famous for its superblades made of high-quality Ludogorie flint, which also attain a wider Balkan distribution. Despite a solid corpus of reliable data for northern Bulgaria from our previous field surveys and laboratory analyses, there are still questions that can only be resolved by further research. This paper presents the results of petrographic and chemical (LA-ICP-MS) analyses of a series of archaeological artefacts and raw material samples collected during a survey in Shumen District of Northeast Bulgaria. These data allow us to i) distinguish two new types of flint (Shumen I and II) which are represented by both raw material outcrops and artefacts and previously referred to as 'Moesian flint'; and ii) expand our analytical data for the Kriva Reka type of Ludogorie flint, confirming its substantial role in prehistoric flint production, distribution and use. These results suggest a more complex network of raw material sources and distribution routes in prehistory than previously assumed.

Hantsche, A. L., K. Kouzmanov, G. Milenkov, S. Vezzoni, R. Vassileva, A. Dini, Th. Sheldrake, O. Laurent, M. Guillong. 2021. Metasomatism and cyclic skarn growth along lithological contacts: Physical and geochemical evidence from a distal Pb-Zn skarn. – *Lithos*; DOI: 10.1016/j.lithos.2021.106408.

Distal skarns form by the metasomatic reactions of a host rock induced by far-traveled hydrothermal fluids. Physical and structural characteristics and geochemical patterns of distal Pb-Zn skarn bodies were studied at the Petrovitsa deposit in Southern Bulgaria. Skarn bodies formed from the interaction of hydrothermal fluid with reactive host lithologies (marble and gneiss). These fluids were transported along sub-vertical feeder structures and lithological contacts. Epidote skarn developed in gneiss protolith, and pyroxene (johannsenite) skarn developed in marble. Detailed geological mapping, complimented by measurements of the internal structure of the skarn body using pyroxene growth versors, quantifies the propagation direction of the skarn body: 1) away from the major local fluid conduit (feeder structure), and 2) away from lithological contacts between aluminosilicate rock and marble. Such growth suggests that fluid flow was generally orthogonal to the skarn front propagation direction in the pyroxene skarn. Textural, mineralogical and geochemical data of skarn samples reveal multiple generations of the major skarn calc-silicates epidote and pyroxene. The epidote skarn is characterized by limited spatial distribution and fine-grained epidote/clinozoisite growth associated with massive replacement and sulfide mineralization. The pyroxene skarn consists of acicular clinopyroxene crystals which form spheroidal aggregates with discrete growth banding. These bands are the physical representation of the cyclic fluid pulses which resulted in rhythmic skarn growth marked by geochemical banding. In situ geochemical analyses in the epidote skarn reveal early Al-rich epidote overprinted by Fe-rich epidote associated with higher Mn and Sr contents and irregular compositional banding. Clinopyroxene ($Jo_{60–95}$) shows general increase in Na, Al, Mn, and REE+Y with distance from the feeder structure and lithologic contacts. These elements correlate with the distance traveled by the hydrothermal fluid from the feeder to the site of skarnification, which we define using a proxy based on the Al content of pyroxene crystals. This reflects an increasing degree of fluid "contamination" by interaction with the aluminosilicate host rocks and functions as a proxy for fluid transport distance. The spatial distribution of trace-elements in pyroxene on an outcrop scale is indicative of discrete pulses of hydrothermal fluid resulting in precipitation of skarn calc-silicates along the increasingly tortuous fluid pathway between the feeder structure and the skarn front, resulting in both the macro- and microscale chemical and textural variability of the skarn body.

Kołodziej, B., D. Ivanova. 2021. Microencruster-microbial-cement framework of the Upper Jurassic reef developed on the slope of the intra-Tethyan carbonate platform (Bulgaria). – In: *Proceedings of the Geologists' Association*, *132*, 2, 158–169; https://doi.org/10.1016/j.pgeola.2020.10.007.

The carbonate succession in the Lyalintsi section of the western Moesian Platform (Western Bulgaria) displays a shallowing-upward trend. Growth of the Tithonian–Valanginian coral biostromes and low-relief bioherms was preceded by Oxfordian–Kimmeridgian sedimentation of fine-grained peloidal-bioclastic limestones and *Saccocoma*-bearing limestones on the homoclinal ramp and the carbonate platform slope. In the late Kimmeridgian, boundstones with very rare corals, but with easily recognisable biohermal morphology, were developed. The main components of this reef are encrusting microorganisms, microbial crusts and synsedimentary cements. Microencrusters *Labes atramentosa, Crescentiella morronensis, Perturbatacrusta leini* and *Radiomura cautica*, as well as thin crusts of calcified sponges (sclerosponges), are the main biotic components. Corals (almost exclusively microsolenids) are sparse, whereas photophilic microencrusters (e.g., "*Lithocodium–Bacinella"*), are absent, although they are common in the overlying shallow-water part of the Lyalintsi sequence. Microbialites and synsedimentary cements provided additional support for the reef framework. The framework, especially the biotic components, and the reefal facies position within the sedimentary succession, implies that the high-energy upper slope of the carbonate platform was the depositional setting of the microencruster-microbial-cement reef studied. Encrusting microorganisms, except for *C. Morronensis* and sponges, are only known from the intra-Tethyan platforms. This study supports conclusion of studies of coeval Alpine reefs that the presence of the microencruster-microbial-cement framework provides insight into the palaeobathymetry, palaeogeography and tectonic configuration of the intra-Tethyan carbonate platforms.

Korzhenkov, A. M., A. Minchev, V. Tenekedjiev, A. N. Ovschenko, O. V. Dimitrov, A. S. Lar'kov, E. A. Rogozhin, B. Rangelov, A. Strelnikov. 2021. Seismic deformations in an early christian monastery in the area of Djanavara, Varna, Bulgaria. Part 2: Results of investigations. – *Seismic Instruments*, *57* (4), 472–489; DOI: 10.3103/S0747923921040071.

We conducted archaeoseismological studies at the Djanavara Monastery Complex in 2019. It consists of early medieval buildings of different ages, the main of which was the church. The church and the atrium were first badly damaged and then destroyed. There were attempts to repair them, as evidenced by the laying of a doorway in the north wall of the atrium. The age of this seismic event may coincide with the destruction of the "second" Episcopal Basilica of Varna, also built in the second half of the 5th century CE. This earthquake took place several decades later. Judging by the kin-

ematic indicators in the building structures, the source of seismic movements was apparently located N-NE of the Episcopal Basilica of Varna and, accordingly, of the Djanavara Monastery Complex. In this direction, the largest seismotectonic node is located at the intersection of sublatitudinal faults with the Shabla-Kaliakra enseismogenic zone. Subsequent renovation of the Djanavara Church and construction of poor-quality buildings around it took place after this seismic event. However, even in these, later, walls, we see traces of younger seismic deformations, evidenced by numerous buttress walls attached to the walls that survived the second earthquake. Judging by the crepid walls attached to the original meridional walls from the E and W, the seismic movements of the second earthquake propagated along the E-W axis. The third seismic event put an end to the activity of the monastery complex. It can be seen that the repaired low-quality walls were again deformed: the later masonry that covered the doorway moved outward, and there was also a joint deformation of the meridional wall and its buttress. The westward movement of the latest masonry testifies to the source of seismic vibrations of this time, located west of the Djanavara Complex. However, the meridional walls show clockwise rotation of their parts, while a perpendicular wall was rotated counterclockwise. Such a systematic deformation presupposes the location of the seismic source not strictly to the west of the monastery complex, but to the southwest, which coincides with the direction to the source, which we determined for the deformations in the episcopal basilica of Varna. Some researchers believe that the Djanavara Monastery Complex was destroyed and finally abandoned in 614–615 CE during the Avar–Slavic invasion. However, there are materials indicating that residents left ancient Odessos even before the attack, most likely due to a strong (3rd in our case) earthquake, during which the entire city was engulfed in fires and many buildings were destroyed. We were unable to accurately estimate the local seismic intensity for each of the three described ancient earthquakes, however, such significant deformations as systematic inclination and extension of walls, as well as turns of their parts around the vertical axis, indicate that the intensity of seismic vibrations during the studied earthquakes reached IL ≤9 points on the MSK-64 scale. The intensity of seismic vibrations may have been enhanced by unfavorable soil conditions at the site of the construction of the Djanavara Monastery Complex.

Kostova, B., V. Petkova, V. Kostov-Kytin, Y. Tzvetanova, G. Avdeev. 2021. TG/DTG-DSC and high temperature in-situ XRD analysis of natural thaumasite. – *Thermochimica Acta*, *697*, 178863; https://doi.org/10.1016/j.tca.2021.178863.

This paper investigated thermal properties of natural thaumasite, such as phase composition and reaction mechanism of thermal decomposition using simultaneous TG/DTG-DSC in Ar and Air medium up to 1673 K, coupled with masspectrometer for analysis of evolving gases, and in-situ powder X-ray diffraction measurements. The transitional solid phases, grown with increasing of temperature at thaumasite thermal decomposition, are calcium hydrogen carbonate ($Ca(HCO_3)_2$) and hydrogen sulphate ($Ca(HSO_4)_2$), calcite, anhydrite, calcium silicates (wolastonite and larnite), calcium silico-carbonate (spurrite), and calcium silico-sulphate (ternesite). The thermal decomposition in both gaseous media includes the stages of dehydration, dehydroxylation, dacarbonation and desulphuration with obtaining a solid residue of varying degrees of crystallinity. The main solid phase, grown at the highest temperatures, is larnite. Based on the obtained results it was proposed the scheme of chemical reactions, which presents the reaction mechanism of thaumasite thermal decomposition. The defined scheme has both fundamental importance by adding new details of reference data, and practical application for thaumasite identification in chemical archaeology, and in the chemistry of cement and cement-based materials.

Marchev, P., R. Raicheva, S. Georgiev, I. P. Savov, D. Jelev. 2021. Formation of ultrapotassic magma via crustal contamination and hybridization of mafic magma: an example from the Stomanovo monzonite, Central Rhodope Massif, Bulgaria. – *Geol. Mag.* (in press); https://doi.org/10.1017/S0016756821000868.

Generally all orogenic ultra-potassic (U-K) rocks are formed after melting of metasomatised sub-continental lithospheric mantle via subducted crustal mica-bearing lithologies. Here we present another possible model, based on the study of the small Stomanovo U-K monzonite porphyry intrusion in the Central Rhodope Massif, Bulgaria. The monzonite dated at 30.50±0.48 Ma is intruded into the voluminous Oligocene (31.63±0.40 Ma) Bratsigovo-Dospat ignimbrite. The monzonite hosts both normally- and reversely-zoned clinopyroxene (Cpx) phenocrysts. The normally-zoned Cpx is characterized by gradually diminishing core-to-rim Mg# (89–74), whereas the reversely-zoned Cpx has green Fe-rich cores (Mg# 78–55) mantled by normally-zoned Cpx (Mg #87–74). Neither the core of the normally-zoned Cpx, nor the Fe-rich green cores are in equilibrium with the host monzonite. This U-K monzonite shows more radiogenic Sr isotopes [($^{87}Sr/^{86}Sr$)i =0.71066] and εNd(t) = (-7.8 to -8.0) that are distinct from the host ignimbrites with ($^{87}Sr/^{86}Sr$) i = (0.70917–0.70927) and εNd(t)= (-4.6 – -6.5). The Sr-Nd isotopic data and the presence of copious zircon xenocrysts from the underlying metamorphic basement suggest extensive crustal assimilation. Our observations indicate that the Stomanovo U-K monzonite formed after extensive lower or middle crustal fractional crystallization from an evolved magma producing cumulates. The process was followed by hybridization with primitive mantle-derived magma and subsequent continuous crustal contamination. We suggest that instead of inheriting their high K_2O and LILE enrichments from slab-derived/

metasomatic fluids, the Stomanovo U-K monzonite may owe some of its unusually high alkalinity to the assimilation of potassium-rich phases from the Rhodope Massif basement rocks.

Peycheva, I., A. von Quadt, V. Kostov-Kytin, M. Kadiyski, M. Stavrev. 2021. U-Pb dating and composition of columbite from Vishteritsa: Implication for timing of granite magmatism and rare-element granitic pegmatites in the Western Rhodopes, Bulgaria. – *Geologica Carpathica*, *72*, 3, 195–212; https://doi.org/10.31577/GeolCarp.72.3.2.

The economic significance of pegmatites as a source of strategic rare metals for high-tech products and green energy motivated the present study on Ta-Nb oxides from Vishteritsa rare-element beryl-columbite LCT pegmatites of the Rila-West Rhodopes batholith in the Western Rhodopes, Bulgaria. Here, we present the first U/Pb age data from columbite with application of the LA-ICP-MS U-Pb technique and a new X36 columbite standard reference material. The obtained Concordia age of 47.57± 0.32 Ma with a small spread of the individual $^{206}Pb/^{238}U$ ages between 45 and 51.3 Ma argues for early Eocene magmatism and pegmatite formation. The host granite of the rare-element pegmatites is dated 51.94±0.61 Ma with LA-ICP-MS U-Pb technique on zircon and suggests a fertile early Eocene magmatic period in the Western Rhodopes. EPMA data for the composition of the columbite is used to refine the formula of the mineral $(Mn_{0.554}\ Fe_{0.427}\ U_{0.006})_{0.987}(N_{b1.826}\ Ta_{0.085}\ Ti_{0.116})_{2\cdot03}O_6$ and define it as columbite-(Mn). Application of the in-situ LA-ICP-MS data technique establishes a series of typical trace elements (Ti, U, Zr, Hf, Y, W, and Zn) that are usually found in content above 500 ppm. The studied columbite is enriched in heavy rare earth elements (HREE sum: 306–697 ppm) and depleted in light REE and Eu. These geochemical characteristics are collectively interpreted as evidence for crystallization from highly fractionated fluid-rich magma. High UO_2 content reaching 0.89 wt% is characteristic for the Vishteritsa columbite. The decrease of U proximal to cracks and in outer crystal zones documents U-mobility during overprinting hydrothermal processes.

Sałacińska, A., I. Gerdjikov, A. Gumsley, K. Szopa, D. Chew, A. Gawęda, I. Kocjan. 2021. Two stages of Late Carboniferous to Triassic magmatism in the Strandja Zone of Bulgaria and Turkey. – *Geol. Mag.*; https://doi.org/10.1017/S0016756821000650.

Although Variscan terranes have been documented from the Balkans to the Caucasus, the southeastern portion of the Variscan Belt is not well understood. The Strandzha Zone along the border between Bulgaria and Turkey encompasses one such terrane linking the Balkanides and the Pontides. However, the evolution of this terrane, and the Upper Carboniferous to Triassic granitoids within it, is poorly resolved. Here we present laser ablation – inductively coupled plasma – mass spectrometry (LA-ICP-MS) U-Pb zircon ages, coupled with petrography and geochemistry from the Izvorovo pluton within the Sakar Unit (Strandzha Zone). This pluton is composed of variably metamorphosed and deformed granites which yield crystallization ages of *ca.* 251–256 Ma. These ages are older than the previously assumed age of the Izvorovo pluton based on a postulated genetic relationship between the Izvorovo pluton and Late Jurassic to Early Cretaceous metamorphism. A better understanding of units across the Strandzha Zone can now be achieved, revealing two age groups of plutons within it. An extensive magmatic episode occurred *ca.* 312–295 Ma, and a longer-lived episode between *ca.* 275 and 230 Ma. Intrusions associated with both magmatic events were emplaced into pre-Lower Carboniferous basement, and were overprinted by early Alpine metamorphism and deformation. These two stages of magmatism can likely be attributed to changes in tectonic setting in the Strandzha Zone. Such a change in tectonic setting is likely related to the collision between Gondwana-derived terranes and Laurussia, followed by either subduction of the Palaeo-Tethys Ocean beneath Laurussia or rifting in the southern margin of Laurussia, with granitoids forming in different tectonic environments.

Zagorchev, I. 2021. Geology of the Balkan Peninsula. – In: Alderton, D., S. A. Elias (Eds). *Encyclopedia of Geology.* 2nd ed., vol. 4. Elsevier, 382–407; DOI: 10.1016/B978-0-08-102908-4.00056-4

The structure of the Balkan Peninsula is dominated by the Alpine (Alpidic) mountain chains: Carpathians-Balkan (Stara planina), Serbo-Macedonian-Rhodopes, and Dinarian-Albanian-Hellenic. These contain fragments from Precambrian (mostly late Neoproterozoic) and Paleozoic tectonometamorphic units that underwent strong reworking during the Hercynian and the Alpine orogenies. The Alpine evolution was controlled by the Tethyan Vardar ocean and by the pre-existing Variscan structure. The evolution of the Vardar ocean is characterized by Triassic rifting, subsequent opening in Jurassic times, complex periods of subduction and obduction, with closure in Late Jurassic times (producing the Vardar suture), and sealing by Cretaceous and Cenozoic sediments. To the East of the Vardar ocean, shallow seas covered the Moesian platform and its southwestern margins where arc basins developed, such as the Late Jurassic–Early Cretaceous Nish-Troyan trough and the Late Cretaceous volcanic arc with the Timok-Srednogorie basin. The Balkanide and Carpathian fold and thrust belts developed from these arc basins by north-vergent folding, thrusting and uplift in several phases, the most important being of mid-Cretaceous ("Austrian"), latest Cretaceous ("Laramide"), mid-Eocene, and early Miocene times. A second belt, composed mostly of pre-Alpine crustal fragments (Morava-Rhodope belt) is situated between the

Carpathian-Balkanides belts to the east and north, and the Vardar suture, to the west and south. The principal elements of this belt are the Serbo-Macedonian and the Rhodopes massifs. The thrust structures of the Morava-Rhodope have centrifugal vergences. The belt is correlated with the Carpathian Suprageticum. West of the present-day Vardar suture, the Vardar ocean covered the margins of the Apulian (Adriatic) platform where the Dinarides-Albanides-Hellenides (DAH) fold and thrust belt was formed from intense Alpine deformation, beginning in Late Jurassic times in the internal zones (Vardarides, Internal DAH), and continuing in several phases until Miocene times. Deformation migrated westwards, and west-vergent nappe piles moved westwards from the root areas. Thus, the ophiolite massifs and ophiolitic mélanges of the Ophiolitic belt (Internal DAH) are usually regarded as originating from the Vardar ocean floor that was detached and traveled as thrust sheets above the Pelagonian massif to reach the Pindos basin. An alternative concept considers them as products of a second, Pindos, oceanic floor.

Žák, J., M. Svojtka, I. Gerdjikov, A. Kounov, D. A. Vangelov. 2021. The Balkan terranes: a missing link between the eastern and western segments of the Avalonian–Cadomian orogenic belt? – *Intern. Geol. Review*; DOI: 10.1080/00206814.2020.1861486.

The Alpine-Himalayan collision zone involves a number of crustal fragments that originated in the Neoproterozoic to Cambrian Avalonian–Cadomian belt of northern Gondwana. We use the detrital zircon U-Pb geochronology to examine four of these lithotectonic units, now exposed in the Balkans in Bulgaria and Serbia. The obtained age spectra suggest that the Diabase-Phyllitoid Complex (the maximum depositional age, MDA, estimated at 540+5/–9 Ma) was presumably an accretionary wedge or a forearc basin sourced from a nearby volcanic arc, however, its paleo-position remains uncertain. The Vlasina Complex (MDA of 577+5/–6 Ma) was the most "westerly" terrane, adjacent to the Trans-Saharan belt, whereas the Sredna Gora and Stara Planina complexes (MDAs of 546±7 Ma and 579+4/–5, respectively) were positioned next to the Saharan Metacraton and Arabian-Nubian shield. To put the Balkan terranes into a broad context, we statistically compare the detrital zircon ages in other terranes from the Eastern Alps to Iran with igneous and metamorphic U-Pb zircon ages from North African source areas. The statistical comparison is done through multi-dimensional scaling (MDS), a more rigorous method than a visual comparison of age spectra, to examine the degree of inter-sample similarity. This information is then transferred to a tentative paleogeographic map showing position of each terrane with respect to its most likely source region. As a result, we define a "westerly" terrane assemblage, characterized by Mesoproterozoic ages and sourced from the West African craton and the Trans-Saharan belt and an "easterly" assemblage formed next to the Saharan Metacraton and the Arabian-Nubian shield. The present-day position of some of these terranes implies significant dextral strike-slip displacement, perhaps due to movement on the Pangea megashear during the Carboniferous and Permian.